



1 **Characterization of the light absorbing properties, chromophores composition**
2 **and sources of brown carbon aerosol in Xi'an, Northwest China**

3 Wei Yuan^{1,2}, Ru-Jin Huang^{1,3}, Lu Yang¹, Jie Guo¹, Ziyi Chen⁴, Jing Duan^{1,2}, Meng Wang^{1,2}, Ting
4 Wang^{1,2}, Haiyan Ni¹, Yongming Han¹, Yongjie Li⁵, Qi Chen⁶, Yang Chen⁷, Thorsten Hoffmann⁸,
5 Colin O'Dowd⁹

6 ¹State Key Laboratory of Loess and Quaternary Geology, Center for Excellence in Quaternary
7 Science and Global Change, Chinese Academy of Sciences, and Key Laboratory of Aerosol
8 Chemistry & Physics, Institute of Earth Environment, Chinese Academy of Sciences, Xi'an
9 710061, China

10 ²University of Chinese Academy of Sciences, Beijing 100049, China

11 ³Institute of Global Environmental Change, Xi'an Jiaotong University, Xi'an 710049, China

12 ⁴Royal School of Mines, South Kensington Campus, Imperial College London, Exhibition
13 Road, London SW7 3RW, United Kingdom

14 ⁵Department of Civil and Environmental Engineering, Faculty of Science and Technology,
15 University of Macau, Taipa, Macau 999078, China

16 ⁶State Key Joint Laboratory of Environmental Simulation and Pollution Control, College of
17 Environmental Sciences and Engineering, Peking University, Beijing 100871, China

18 ⁷Chongqing Institute of Green and Intelligent Technology, Chinese Academy of Sciences,
19 Chongqing 400714, China

20 ⁸Institute of Inorganic and Analytical Chemistry, Johannes Gutenberg University Mainz,
21 Duesbergweg 10–14, Mainz 55128, Germany

22 ⁹School of Physics and Centre for Climate and Air Pollution Studies, Ryan Institute, National
23 University of Ireland Galway, University Road, Galway H91CF50, Ireland

24 *Correspondence to:* Ru-Jin Huang (rujin.huang@ieecas.cn)

25 **Abstract**

26 The impact of brown carbon aerosol (BrC) on the Earth's radiative forcing balance has



27 been widely recognized but remains uncertain, mainly because the relationships among BrC
28 sources, chromophores, and optical properties of aerosol are poorly understood. In this work,
29 the light absorption properties and chromophore composition of BrC were investigated for
30 samples collected in Xi'an, Northwest China from 2015 to 2016. Both absorption Ångström
31 exponent and mass absorption efficiency show distinct seasonal differences, which could be
32 attributed to the differences in sources and chromophore composition of BrC. Three groups of
33 light-absorbing organics were found to be important BrC chromophores, including those show
34 multiple absorption peaks at wavelength > 350 nm (12 polycyclic aromatic hydrocarbons and
35 their derivatives) and those show single absorption peak at wavelength < 350 nm (10
36 nitrophenols and nitrosalicylic acids and 3 methoxyphenols). These measured BrC
37 chromophores show distinct seasonal differences and contribute on average about 1.1% and 3.3%
38 of light absorption of methanol-soluble BrC at 365 nm in summer and winter, respectively,
39 about 7 and 5 times higher than the corresponding carbon mass fractions in total organic carbon.
40 The sources of BrC were resolved by positive matrix factorization (PMF) using these
41 chromophores instead of commonly used non-light absorbing organic markers as model inputs.
42 Our results show that in spring vehicular emissions and secondary formation are major sources
43 of BrC (~70%), in fall coal combustion and vehicular emissions are major sources (~70%), in
44 winter biomass burning and coal combustion become major sources (~80%), while in summer
45 secondary BrC dominates (~60%).

46 **1 Introduction**

47 Brown carbon (BrC) is an important component of atmospheric aerosol particles and has
48 significant effects on radiative forcing and climate (Feng et al., 2013; Laskin et al., 2015; Zhang
49 et al., 2017a). BrC can efficiently absorb solar radiation and reduce the photolysis rates of
50 atmospheric radicals (Jacobsan, 1999; Li et al., 2011; Mok et al., 2016), which ultimately
51 influences the atmospheric photochemistry process, the formation of secondary organic aerosol
52 (SOA), and therefore the regional air quality (Mohr et al., 2013; Laskin et al., 2015; Moise et
53 al., 2015). In addition, some components in BrC, such as nitrated aromatic compounds (NACs)
54 (Teich et al., 2017; Wang et al., 2018) and polycyclic aromatic hydrocarbons (PAHs)
55 (Samburova et al., 2016; Huang et al., 2018), have adverse effects on human health. The



56 significant effects of BrC on environment, climate, air quality and living things call for more
57 studies to understand its chemical characteristics, sources and the links with optical properties.

58 Investigating the chemical composition of BrC at molecular level is necessary, because
59 even small amounts of compounds can have a significant effect on the light absorption
60 properties of BrC and profound atmospheric implication (Mohr et al., 2013; Zhang et al., 2013;
61 Teich et al., 2017; Huang et al., 2018). A number of studies have investigated the BrC
62 composition at molecular level (Mohr et al., 2013; Zhang et al., 2013; Chow et al., 2015;
63 Samburova et al., 2016; Lin et al., 2016, 2017, 2018; Teich et al., 2017; Huang et al., 2018; Lu
64 et al., 2019). For example, Zhang et al. (2013) measured 8 NACs in Los Angeles and found that
65 they contributed about 4% of water-soluble BrC absorption at 365 nm. Huang et al. (2018)
66 measured 18 PAHs and their derivatives in Xi'an and found that they accounted for on average
67 ~1.7% of the overall absorption of methanol-soluble BrC. A state-of-the-art high performance
68 liquid chromatography-photodiode array-high resolution mass spectrometry (HPLC-PDA-
69 HRMS) was applied to investigate the elemental composition of BrC chromophores in biomass
70 burning aerosol (Lin et al., 2016, 2017, 2018). Despite these efforts, the molecular composition
71 of atmospheric BrC still remains largely unknown due to its complexity in emission sources
72 and formation processes.

73 Field observations and laboratory studies show that BrC has various sources, including
74 primary emissions such as combustion and secondary formation from various atmospheric
75 processes (Laskin et al., 2015). Biomass burning, including forest fires and burning of crop
76 residues, is considered as the main source of BrC (Teich et al., 2017; Lin et al., 2017). Coal
77 burning and vehicle emissions are also important primary sources of BrC (Yan et al., 2017; Xie
78 et al., 2017). Secondary BrC is produced through multiple-phase reactions occurring in or
79 between gas phase, particle phase, and cloud droplets. For example, nitrification of aromatic
80 compounds (Harrison et al., 2005; Lu et al., 2011), oligomers of acid-catalyzed condensation
81 of hydroxyl aldehyde (De Haan et al., 2009; Shapiro et al., 2009), and reaction of ammonia
82 (NH₃) or amino acids with carbonyls (De Haan et al., 2011; Nguyen et al., 2013; Flores et al.,
83 2014) can all produce BrC. Condensed phase reactions and aqueous-phase reactions have also
84 been found to be important formation pathways for secondary BrC in ambient air (Gilardoni et



85 al., 2016). In addition, atmospheric aging processes can lead to either enhancement or bleaching
86 of the BrC absorption (Lambe et al., 2013; Lee et al., 2014; Zhong and Jang, 2014), further
87 challenging the characterization of BrC.

88 As the starting point of the Silk Road, Xi'an is an important inland city in northwestern
89 China experiencing severe particulate air pollution, especially during heating period with
90 enhanced coal combustion and biomass burning activities (Wang et al., 2016; Ni et al., 2018).
91 In this study, we performed spectroscopic measurement and chemical analysis of PM_{2.5} filter
92 samples in Xi'an to investigate: 1) seasonal variations in the light absorption properties and
93 chromophore composition of BrC, and their relationships; 2) sources of BrC in different seasons
94 based on positive matrix factorization (PMF) model with light-absorbing organic markers as
95 input species.

96 **2 Experimental**

97 **2.1 Aerosol sampling**

98 A total of 112 daily ambient PM_{2.5} filter samples were collected on pre-baked (780 °C, 3
99 h) quartz-fiber filters (20.3 × 25.4 cm, Whatman, QM-A) in November-December 2015, April-
100 May, July, October-November 2016, representing winter, spring, summer and fall, respectively.
101 Filter samples were collected using a Hi-Vol PM_{2.5} air sampler (Tisch, Cleveland, OH) at a flow
102 rate of 1.05 m³ min⁻¹ on the roof (~10 m above ground level, 34.22°N, 109.01°E) of the Institute
103 of Earth Environment, Chinese Academy of Sciences, which was surrounded by residential
104 areas without large industrial activities. After collection, the filter samples were wrapped in
105 baked aluminum foils and stored in a freezer (-20 °C) until further analysis.

106 **2.2 Light absorption measurement**

107 One punch of loaded filter (0.526 cm²) was taken from each sample and sonicated for 30
108 minutes in 10 mL of ultrapure water (> 18.2 MΩ · cm) or methanol (J. T. Baker, HPLC grade).
109 The extracts were then filtered with a 0.45 μm PTFE pore syringe filter to remove insoluble
110 materials. The light absorption spectra of water-soluble and methanol-soluble BrC were
111 measured with an UV-Vis spectrophotometer (300-700 nm) equipped with a liquid waveguide
112 capillary cell (LWCC-3100, World Precision Instrument) following the method by Hecobian et



113 al. (2010). The measured absorption data can be converted to the absorption coefficient by
114 equation (1):

$$115 \quad \text{Abs}_\lambda = (A_\lambda - A_{700}) \frac{V_f}{V_a \times L} \times \ln(10) \quad (1)$$

116 where A_{700} is the absorption at 700 nm, serving as a reference to account for baseline drift, V_f
117 is the volume of water or methanol that the filter was extracted into, V_a is the volume of sampled
118 air, L is the optical path length (0.94 m). A factor of $\ln(10)$ is used to convert the log base-10
119 (recorded by UV-Vis spectrophotometer) to natural logarithm to provide base-e absorption
120 coefficient. The absorption coefficient of water-soluble or methanol-soluble organics at 365 nm
121 (Abs_{365}) is used to represent water-soluble or methanol-soluble BrC absorption, respectively.

122 The mass absorption efficiency (MAE) of BrC in the extracts can be calculated as:

$$123 \quad \text{MAE}_\lambda = \frac{\text{Abs}_\lambda}{M} \quad (2)$$

124 where M ($\mu\text{gC m}^{-3}$) is the concentration of water-soluble organic carbon (WSOC) for water
125 extracts or methanol-soluble organic carbon (MSOC) for methanol extracts. Note that organic
126 carbon (OC) is often used to replace MSOC because direct measurement of MOSC is
127 technically difficult and many studies have shown that most of OC (~ 90%) can be extracted
128 by methanol (Chen and Bond, 2010; Cheng et al., 2016; Xie et al., 2019).

129 The wavelength-dependent light absorption of chromophores in solution, termed as
130 absorption Ångström exponent (AAE), can be described as:

$$131 \quad \text{Abs}_\lambda = K \cdot \lambda^{-\text{AAE}} \quad (3)$$

132 where K is a constant related to the concentration of chromophores and AAE is calculated by
133 linear regression of $\log \text{Abs}_\lambda$ versus $\log \lambda$ in the wavelength range of 300-410 nm.

134 2.3 Chemical analysis

135 OC was measured with a thermal/optical carbon analyzer (DRI, model 2001) following
136 the IMPROVE-A protocol (Chow et al., 2011). WSOC was measured with a TOC/TN analyzer
137 (TOC-L, Shimadzu, Japan) (Ho et al., 2015).

138 Organic compounds listed in Table S1 were analyzed with a gas chromatograph-mass
139 spectrometer (GC-MS). The concentrations of NACs were analyzed following the method by
140 Al-Naiema and Stone (2017). Briefly, a quarter of 47 mm filter sample was ultrasonically



141 extracted with 2 mL of methanol for 15 minutes and repeated three times. 4-Nitrophenol-
142 2,3,5,6-d₄ was added as an internal standard before extraction to correct for potential loss of
143 analytes during the extraction process. The extracts were filtered with a 0.45 μm PTFE syringe
144 filter and then evaporated with a rotary evaporator to ~1 mL and dried with a gentle stream of
145 nitrogen. Then, 50 μL of N,O-bis(trimethylsilyl)trifluoroacetamide (BSTFA-TMCS; Fluka
146 Analytical 99%) and 10 μL of pyridine were added. The mixture was heated for 3 h at 70 °C for
147 silylation. After reaction, 140 μL of n-hexane were added to dilute the derivatives. Finally, 2 μL
148 aliquot of the derivatized extracts were introduced into the GC-MS, which was equipped with
149 a DB-5MS column, electron impact (EI) ionization source (70 eV), and a GC inlet of 280 °C.
150 The GC oven temperature was held at 50 °C for 2 min, increased from 50 °C to 120 °C at a rate
151 of 15 °C min⁻¹, then further increased from 120 °C to 300 °C at a rate of 10 °C min⁻¹ for a total
152 running time of 25 min. The concentrations of PAHs and its oxygenated derivatives,
153 methoxyphenols (MOPs), levoglucosan, hopanes and phthalic acid were analyzed following
154 methods described by Wang et al. (2006).

155 **2.4 Source apportionment of BrC**

156 Source apportionment of methanol-soluble BrC was performed using positive matrix
157 factorization (PMF) as implemented by the multilinear engine (ME-2; Paatero, 1997) via the
158 Source Finder (SoFi) interface written in Igor Wavemetrics (Canonaco et al., 2013). Abs_{365,MSOC}
159 and those light-absorbing species including fluoranthene (FLU), pyrene (PYR), chrysene
160 (CHR), benzo(a)anthracene (BaA), benzo(a)pyrene (BaP), benzo(b)fluoranthene (BbF),
161 benzo(k)fluoranthene (BkF), indeno[1,2,3-cd]pyrene (IcdP), benzo(ghi)perylene (BghiP), 9,10-
162 anthracenequinone (9,10-AQ), benzanthrone (BEN), benzo[b]fluoren-11-one (BbF11O),
163 vanillic acid, vanillin and syringyl acetone were used as model inputs, together with some non-
164 light absorbing markers, i.e., phthalic acid, hopanes (17α(H),21β(H)-30-norhopane,
165 17α(H),21β(H)-hopane, 17α(H),21β(H)-(22S)-homohopane, 17α(H),21β(H)-(22R)-
166 homohopane, referred to as HP1-HP4, respectively), picene, and levoglucosan. The input data
167 include species concentrations and uncertainties. The method detection limits (MDLs),
168 calculated as three times of the standard deviation of the blank filters, were used to estimate
169 species-specific uncertainties, following Liu et al. (2017). Furthermore, for a clear separation



170 of sources profiles, the contribution of corresponding markers was set to 0 in the sources
171 unrelated to the markers (see Table S2).

172 **3 Results and discussion**

173 **3.1 Light absorption properties of water- and methanol-soluble BrC**

174 Fig. 1 shows the temporal profiles of Abs_{365} of water- and methanol-soluble BrC, together
175 with the concentrations of WSOC and OC (representing MSOC). They all show similar
176 seasonal variations with the highest average in winter, followed by fall, spring and summer (see
177 Table S3). WSOC contributed annually $54.4 \pm 16.2\%$ of the OC mass, with the highest
178 contribution in summer ($66.1 \pm 15.5\%$) and the lowest contribution in winter ($45.1 \pm 10.2\%$).
179 The higher WSOC fraction in OC during summer may be related to biomass burning emissions
180 and SOA formation which produce more WSOC (Ram et al., 2012; Yan et al., 2015). The lower
181 WSOC fractions in OC during winter could be attributed to enhanced emissions from coal
182 combustion and motor vehicles which produce a large fraction of water-insoluble organics (Dai
183 et al., 2015; Daellenbach et al., 2016; Yan et al., 2017). $Abs_{365,MSOC}$ is approximately 2 times
184 (range 1.7-2.3) higher than $Abs_{365,WSOC}$, which is similar to the results measured in Beijing
185 (Cheng et al., 2016), southeastern Tibetan Plateau (Zhu et al., 2018), Gwangju, Korea (Park et
186 al., 2018) and the Research Triangle Park, USA (Xie et al., 2019), indicating that the optical
187 properties of BrC could be largely underestimated when using water as the extracting solvent.
188 In Fig. S1 we summarized those previously reported $Abs_{365,WSOC}$ (as $Abs_{365,MSOC}$ was not
189 commonly measured in many previous studies) values at different sites in Asian urban and
190 remote areas and the US. $Abs_{365,WSOC}$ is significantly higher in most Asian urban regions than
191 in the Asian remote sites and the US, and show clear seasonal variations. The high light
192 absorption of BrC in Asian urban regions, especially during winter, may have important effects
193 on regional climate and radiation forcing (Park et al., 2010; Laskin et al., 2015). As discussed
194 in Feng et al. (2013), the average global climate forcing of BrC was estimated to be 0.04-0.11
195 $W m^{-2}$ and above $0.25 W m^{-2}$ in urban sites of south and east Asia regions, which is about 25%
196 of the radiative forcing of black carbon (BC, $1.07 W m^{-2}$). Thus, to further understand the
197 influence of BrC on regional radiation forcing, it is essential to identify and quantify the sources



198 of BrC in Asia.

199 The seasonal averages of AAE of water-soluble BrC were between 5.32 and 6.15 without
200 clear seasonal trend (see Table S3). The seasonal averages of AAE of methanol-soluble BrC
201 were relatively lower than those of water-soluble BrC, ranging from 4.45 to 5.18 which is
202 similar to the results in Los Angeles Basin (Zhang et al., 2013) and Gwangju, Korea (Park et
203 al., 2018). This is because methanol can extract more compounds with high conjugation degree
204 and strong light-absorbing capability (e.g., PAHs) at longer wavelength (> 350 nm). The AAE
205 values of water-soluble BrC (as AAE of methanol-soluble BrC was not commonly measured in
206 many previous studies) in urban, rural and remote regions show a large difference (see Fig. 2a),
207 typically with much lower AAE values in urban regions than those in rural and remote regions,
208 indicating the difference in sources and chemical composition of chromophores. The urban
209 regions are mainly affected by anthropogenic emissions. Therefore, urban BrC may contain a
210 large amount of aromatic chromophores with high conjugation degree, which absorb light at a
211 longer wavelength and have lower AAE values (Lambe et al., 2013; Wang et al., 2018).

212 The average MAE_{365} values of water- and methanol-soluble BrC show large seasonal
213 variations, with higher values in winter (1.85 and 1.50 $m^2 gC^{-1}$, respectively) and fall (1.18 and
214 1.52 $m^2 gC^{-1}$), and lower values in spring (1.01 and 0.79 $m^2 gC^{-1}$) and summer (0.91 and 1.21
215 $m^2 gC^{-1}$). Such large seasonal differences indicate seasonal difference in BrC sources, as
216 discussed below. Compared to previous studies (Fig. 2b), the average values of $MAE_{365,WSOC}$
217 are obviously higher in urban sites than in rural and remote sites. The higher $MAE_{365,WSOC}$
218 values in urban regions is likely associated with enhanced anthropogenic emissions from e.g.,
219 coal combustion and biomass burning, and the lower $MAE_{365,WSOC}$ values in rural and remote
220 regions could be attributed to biogenic sources or aged secondary BrC (Lei et al., 2018; Xie et
221 al., 2019).

222 3.2 Chemical characterization of the BrC chromophores

223 Given the complexity in emission sources and formation processes, the molecular
224 composition of atmospheric BrC remains largely unknown. PAHs, NACs and MOPs have
225 recently been found as major chromophores in biomass burning-derived BrC (Lin et al., 2016,
226 2017, 2018). However, these compounds can also be directly emitted by coal combustion and



227 motor vehicle or formed by secondary reactions (Harrison et al., 2005; Iinuma et al., 2010; Liu
228 et al., 2017; Wang et al., 2018; Lu et al., 2019), making source attribution of atmospheric BrC
229 more challenging. To obtain the exact molecular composition of BrC chromophores and
230 understand the influence of a specific chromophore on BrC optical property, we measured the
231 light absorption characteristics of available chromophore standards including 12 PAHs, 10
232 NACs and 3 MOPs, and quantified their concentrations in PM_{2.5} samples with GC-MS. The
233 light absorption contribution of individual chromophores to that of methanol-soluble BrC in the
234 wavelength range of 300-500 nm was estimated according to its concentration and mass
235 absorption efficiency (see Supplementary). Fig. 3 shows the contribution of carbon content in
236 identified BrC chromophores to the total OC mass. They all show obvious seasonal variations
237 with the highest values in winter and lowest in summer. The seasonal difference can be up to a
238 factor of 5-6. The contribution of PAHs ranged from 0.12% in summer to 0.47% in winter,
239 NACs from 0.02% in summer to 0.13% in winter, and MOPs from 0.01% in summer to 0.06%
240 in winter. It should be noted that NACs are dominated by 4-nitrophenol and 4-nitrocatechol in
241 spring, fall and winter, but by 4-nitrophenol and 5-nitrosalicylic acid in summer. The difference
242 is likely due to enhanced summertime formation of 5-nitrosalicylic acid, which is more oxidized
243 than other nitrated phenols measured in this study (Wang et al., 2018).

244 The seasonally averaged contributions of PAHs, NACs, MOPs and total measured
245 chromophores to light absorption of methanol-soluble BrC between 300 to 500 nm are shown
246 in Fig. 4. They show large seasonal variations and wavelength dependence. Specifically, PAHs
247 made the largest contribution to BrC light absorption in autumn, followed by winter, spring and
248 summer, and show two large absorption peaks at about 365 nm and 380 nm, which are mainly
249 associated with the absorption of BaP, BghiP, IcdP, FLU, BkF and BaA (see Fig. S2). Compared
250 to PAHs, NACs show the largest contribution in winter, followed by fall, spring and summer,
251 and exhibit only one absorption peak at about 320 nm in spring and summer and at about 330
252 nm in fall and winter. The red shift in the absorption peak could be attributed to the increase of
253 contributions from 4-nitrocatechol, 4-methyl-5-nitrocatechol and 3-methyl-5-nitrocatechol
254 which have absorption peak at about 330-350 nm (see Fig. S2). Different from PAHs and NACs,
255 MOPs contribute the most in winter, followed by spring, fall and summer, and only show one



256 absorption peak at about 310 nm. The difference in light absorption contributions of different
257 chromophores in different seasons reflects the difference in sources, emission strength and
258 atmospheric formation processes.

259 The total contributions of PAHs, NACs and MOPs to the light absorption of methanol-
260 soluble BrC at 365 nm ranged from 1.05% (summer) to 3.26% (winter) (see Table 1). The
261 average contribution of PAHs to the BrC light absorption at 365 nm was 0.97% in summer (the
262 lowest) and 2.69% in fall (the highest), the contribution of NACs was 0.09% in summer and
263 0.82% in winter, and the contribution of MOPs was 0.006% in summer and 0.024% in winter.
264 The low contributions of these measured chromophores to the light absorption of methanol-
265 soluble BrC are consistent with previous studies. For example, Huang et al. (2018) measured
266 18 PAHs and their derivatives, which on average contributed ~1.7% of the overall absorption
267 of methanol-soluble BrC in Xi'an. Mohr et al. (2013) estimated the contribution of five NACs
268 to particulate BrC light absorption at 370 nm to be ~4% in Detling, UK. Zhang et al. (2013)
269 measured eight NACs, which accounted for ~4% of water-soluble BrC absorption at 365 nm in
270 Los Angeles. Teich et al. (2017) determined eight NACs during six campaigns at five locations
271 in summer and winter, and founded that the mean contribution of NACs to water-soluble BrC
272 absorption at 370 nm ranged from 0.10% to 1.25% under acidic conditions and from 0.13% to
273 3.71% under alkaline conditions. Slightly different from these previous studies, we investigated
274 the contributions of three groups of chromophores with different light-absorbing properties to
275 the light absorption of BrC, and provided further understanding in the relationships between
276 optical properties and chemical composition of BrC in the atmosphere. For example, vanillin,
277 which has negligible contribution to BrC light absorption at 365 nm, can produce secondary
278 BrC through oxidation and thus enhance the light absorption by a factor of 5-7 (Li et al., 2014;
279 Smith et al., 2016). The contribution of PAHs to the light absorption of methanol-soluble BrC
280 at 365 nm was 5-13 times that of their mass fraction of carbon in OC, 6-9 times for NACs, and
281 0.4-0.7 times for MOPs (4-8 times at 310 nm for MOPs). These results further demonstrate that
282 even a small amount of chromophores can have a disproportionately high impact on the light
283 absorption properties of BrC, and that the light absorption of BrC is likely determined by a
284 number of chromophores with strong light absorption ability (Kampf et al., 2012; Teich et al.,



285 2017).

286 3.3 Sources of BrC

287 Two approaches have been used to quantify the sources of BrC, including multiple linear
288 regression and receptor models such as PMF. For example, Washenfelder et al. (2015) utilized
289 multiple linear regression to determine the contribution of individual OA factors resolved by
290 PMF to OA light absorption in the southeastern America. Moschos et al. (2018) combined the
291 time series of PMF-resolved OA factors with the time series of light absorption of water-soluble
292 OA extract as model inputs to quantify the sources of BrC in Magadino and Zurich, Switzerland.
293 Xie et al. (2019) quantified the sources of BrC in southeastern America using Abs_{365} , elemental
294 carbon (EC), OC, WSOC, isoprene sulfate ester, monoterpene sulfate ester, levoglucosan and
295 isoprene SOA tracers as PMF model inputs. However, it should be noted that previous studies
296 mainly rely on the correlation between measured light absorption and organic tracers that do
297 not contain a BrC chromophore, and therefore may lead to bias in BrC source apportionment.
298 To better constrain the sources of BrC (i.e., contribution to $Abs_{365,MSOC}$), we used BrC
299 chromophores as PMF model inputs. The inputs include vanillic acid, vanillin, and syringyl
300 acetone for BrC from biomass burning, and FLU, PYR, CHR, BaA, BaP, BbF, BkF, IcdP, BghiP,
301 9,10AQ, BEN, and BbF11O for BrC from incomplete combustion. In addition, we included
302 non-light absorbing levoglucosan for biomass burning, phthalic acid for secondary BrC,
303 hopanes for vehicle emission and picene for coal burning in the model inputs.

304 Four factors were resolved, including vehicle emission, coal burning, biomass burning and
305 secondary formation. The profile of each factor is shown in Fig. S3. The first factor is
306 characterized by a high contribution of phthalic acid, a tracer of secondary formation of OA.
307 The second factor is dominated by hopanes, mainly from vehicular emissions. The third factor
308 is characterized by high contributions of PI, BaP, BbF, BkF, IcdP, BghiP, mainly from coal
309 combustion emissions, while the fourth factor has high contributions of levoglucosan, vanillic
310 acid, vanillin, syringyl acetone from biomass burning emissions. The seasonal difference in
311 relative contribution of each factor to BrC light absorption is shown in Fig. 5. In spring,
312 vehicular emissions (34%) and secondary formation (37%) were the main contributors to BrC
313 and coal combustion also had a relatively large contribution (29%). In summer, secondary



314 formation constituted the largest fraction (~60%), mainly due to enhanced photochemical
315 formation of secondary BrC. In fall, vehicular emissions (38%), coal combustion (29%) and
316 biomass burning (22%) all had significant contributions to BrC. In winter, coal combustion
317 (44%) and biomass burning (36%) were the main contributors, due to emissions from
318 residential biomass burning (wood and crop residues) and coal combustion for heating. Such
319 large seasonal difference in emission sources and atmospheric processes of BrC indicates that
320 more studies are required to better understand the relationship between chemical composition,
321 formation processes, and light absorption properties of BrC.

322 **4 Conclusion**

323 The light absorption properties of water- and methanol-soluble BrC in different seasons
324 were investigated in Xi'an. The light absorption coefficient of methanol-soluble BrC was
325 approximately 2 times higher than that of water-soluble BrC at 365 nm, and had an average
326 MAE₃₆₅ value of $1.27 \pm 0.46 \text{ m}^2 \text{ gC}^{-1}$. The average MAE₃₆₅ value of water-soluble BrC was 1.19
327 $\pm 0.51 \text{ m}^2 \text{ gC}^{-1}$, which is comparable to those in previous studies at urban sites but higher than
328 those in rural and remote areas. The seasonally averaged AAE values of water-soluble BrC
329 ranged from 5.32 to 6.15, which are higher than those of methanol-soluble BrC (between 4.45
330 and 5.18). In combination with previous studies, we found that AAE values of water-soluble
331 BrC were much lower in urban regions than those in rural and remote regions. The difference
332 of optical properties of BrC in different regions could be attributed to the difference in sources
333 and chemical composition of BrC chromophores. The contributions of 12 PAHs, 10 NACs and
334 3 MOPs to the light absorption of methanol-soluble BrC were determined and showed large
335 seasonal variations. Specifically, the total contribution to methanol-soluble BrC light absorption
336 at 365 nm ranged from 1.1% to 3.3%, which is 5-7 times higher than their carbon mass fractions
337 in total OC. This result indicates that the light absorption of BrC is likely determined by an
338 amount of chromophores with strong light absorption ability. Four major sources of methanol-
339 soluble BrC were identified, including secondary formation, vehicle emission, coal combustion
340 and biomass burning. On average, secondary formation and vehicular emission were the main
341 contributors of BrC in spring (~70%). Vehicular emission (38%), coal burning (29%) and
342 biomass burning (22%) all contributed significantly to BrC in fall. Coal combustion and



343 biomass burning were the major contributors in winter (~80%), and secondary formation was
344 the predominant source in summer (~60%). The large variations of BrC sources in different
345 seasons suggest that more studies are needed to understand the seasonal difference in chemical
346 composition, formation processes, and light absorption properties of BrC, as well as their
347 relationships.

348 **5 Abbreviations of organics**

349 **PAHs (Polycyclic Aromatic Hydrocarbons)**

350	BaA	Benzo(a)anthracene
351	BaP	Benzo(a)pyrene
352	BbF	Benzo(b)fluoranthene
353	BbF11O	Benzo[b]fluoren-11-One
354	BEN	Benzanthrone
355	BghiP	Benzo(ghi)perylene
356	BkF	Benzo(k)fluoranthene
357	CHR	Chrysene
358	FLU	Fluoranthene
359	IcdP	Indeno[1,2,3-cd]pyrene
360	PYR	Pyrene
361	9,10AQ	9,10-Anthracenequinone

362 **NACs (Nitrated Aromatic Compounds)**

363	2M4NP	2-Methyl-4-Nitrophenol
364	2,6DM4NP	2,6-Dimethyl-4-Nitrophenol
365	3M4NP	3-Methyl-4-Nitrophenol
366	3M5NC	3-Methyl-5-Nitrocatechol
367	3NSA	3-Nitrosalicylic Acid
368	4M5NC	4-Methyl-5-Nitrocatechol
369	4NC	4-Nitrocatechol
370	4NP	4-Nitrophenol



371	4N1N	4-Nitro-1-Naphthol
372	5NSA	5-Nitrosalicylic Acid
373	MOP (Methoxyphenols)	
374	SyA	Syringyl Acetone
375	VaA	Vanillic Acid
376	VAN	Vanillin
377	Hopanes	
378	HP1	17 α (H),21 β (H)-30-Norhopane
379	HP2	17 α (H),21 β (H)-Hopane
380	HP3	17 α (H),21 β (H)-(22S)-Homohopane
381	HP4	17 α (H),21 β (H)-(22R)-Homohopane

382 *Data availability.* Raw data used in this study are archived at the Institute of Earth Environment,
383 Chinese Academy of Sciences, and are available on request by contacting the corresponding
384 author.

385 *Supplement.* The Supplement related to this article is available online at

386 *Author contributions.* RJH designed the study. Data analysis was done by WY, LY, and RJH.
387 WY, LY and RJH interpreted data, prepared the display items and wrote the manuscript. All
388 authors commented on and discussed the manuscript.

389 *Acknowledgements.* This work was supported by the National Natural Science Foundation of
390 China (NSFC) under grant no. 41877408 and no. 91644219, the Chinese Academy of Sciences
391 (no. ZDBS-LY-DQC001), the Cross Innovative Team fund from the State Key Laboratory of
392 Loess and Quaternary Geology (SKLLQG) (no. SKLLQGT1801), and the National Key
393 Research and Development Program of China (no. 2017YFC0212701). Yongjie Li
394 acknowledges funding support from the National Natural Science Foundation of China



395 (41675120), the Science and Technology Development Fund, Macau SAR (File no.
396 016/2017/A1), and the Multi-Year Research grant (No. MYRG2018-00006-FST) from the
397 University of Macau.

398 **References**

399 Al-Naiema, I. M., and Stone, E. A.: Evaluation of anthropogenic secondary organic aerosol
400 tracers from aromatic hydrocarbons, *Atmos. Chem. Phys.*, 17, 2053-2065,
401 doi:10.5194/acp-17-2053-2017, 2017.

402 Bosch, C., Andersson, A., Kirillova, E. N., Budhavant, K., Tiwari, S., Praveen, P. S., Russell,
403 L. M., Beres, N. D., Ramanathan, V., and Gustafsson, Ö.: Source-diagnostic dual-isotope
404 composition and optical properties of water-soluble organic carbon and elemental carbon
405 in the South Asian outflow intercepted over the Indian Ocean, *J. Geophys. Res. Atmos.*,
406 119, 11743-11759, doi:10.1002/2014JD022127, 2014.

407 Chen, Y., and Bond, T. C.: Light absorption by organic carbon from wood combustion, *Atmos.*
408 *Chem. Phys.*, 10, 1773-1787, doi:10.5194/acp-10-1773-2010, 2010.

409 Chen, Y., Ge, X., Chen, H., Xie, X., Chen, Y., Wang, J., Ye, Z., Bao, M., Zhang, Y., and Chen,
410 M.: Seasonal light absorption properties of water-soluble brown carbon in atmospheric
411 fine particles in Nanjing, China, *Atmos. Environ.*, 187, 230-240,
412 doi:10.1016/j.atmosenv.2018.06.002, 2018.

413 Cheng, Y., He, K. B., Du, Z. Y., Engling, G., Liu, J. M., Ma, Y. L., Zheng, M., and Weber, R. J.:
414 The characteristics of brown carbon aerosol during winter in Beijing, *Atmos. Environ.*,
415 127, 355-364, doi:10.1016/j.atmosenv.2015.12.035, 2016.

416 Chow, J. C., Watson, J. G., Robles, J., Wang, X. L., Antony Chen, L. W., Trimble, D. L., Kohl,
417 S. D., Tropp, R. J., and Fung, K. K.: Quality assurance and quality control for
418 thermal/optical analysis of aerosol samples for organic and elemental carbon, *Anal.*
419 *Bioanal. Chem.*, 401, 3141- 3152, doi:10.1007/s00216-011-5103-3, 2011.

420 Chow, K. S., Huang, X. H. H., and Yu, J. Z.: Quantification of nitroaromatic compounds in
421 atmospheric fine particulate matter in Hong Kong over 3 years: field measurement
422 evidence for secondary formation derived from biomass burning emissions, *Environ.*
423 *Chem.*, 13, 665-673, doi:10.1071/EN15174, 2015.



- 424 Canonaco, F., Crippa, M., Slowik, J. G., Baltensperger, U., and Prévôt, A. S. H.: SoFi, an IGOR
425 based interface for the efficient use of the generalized multilinear engine (ME-2) for the
426 source apportionment: ME-2 application to aerosol mass spectrometer data, *Atmos. Meas.*
427 *Tech.*, 6, 3649-3661, doi:10.5194/amt-6-3649-2013, 2013.
- 428 Daellenbach, K. R., Bozzetti, C., Krepelova, A. K., Canonaco, F., Wolf, R., Zotter, P., Fermo,
429 P., Crippa, M., Slowik, J. G., Sosedova, Y., Zhang, Y., Huang, R. J., Poulain, L., Szidat, S.,
430 Baltensperger, U., El Haddad, I., and Prevot, A. S. H.: Characterization and source
431 apportionment of organic aerosol using offline aerosol mass spectrometry, *Atmos. Meas.*
432 *Tech.*, 9, 23-39, doi:10.5194/amt-9-23-2016, 2016.
- 433 Dai, S., Bi, X., Chan, L., He, J., Wang, B., Wang, X., Peng, P., Sheng, G., and Fu, J.: Chemical
434 and stable carbon isotopic composition of PM_{2.5} from on-road vehicle emissions in the
435 PRD region and implications for vehicle emission control policy, *Atmos. Chem. Phys.*, 15,
436 3097-3108, doi:10.5194/acp-15-3097-2015, 2015.
- 437 De Haan, D. O., Corrigan, A. L., Smith, K. W., Stroik, D. R., Turley, J. J., Lee, F. E., Tolbert,
438 M. A., Jimenez, J. L., Cordova, K. E., and Ferrell, G. R.: Secondary organic aerosol-
439 forming reactions of glyoxal with amino acids, *Environ. Sci. Technol.*, 43, 2818-2824,
440 doi:10.1021/es803534f, 2009.
- 441 De Haan, D. O., Hawkins, L. N., Kononenko, J. A., Turley, J. J., Corrigan, A. L., Tolbert, M.
442 A., and Jimenez, J. L.: Formation of nitrogen-containing oligomers by methylglyoxal and
443 amines in simulated evaporating cloud droplets, *Environ. Sci. Technol.*, 45, 984-991,
444 doi:10.1021/es102933x, 2011.
- 445 Feng, Y., Ramanathan, V., and Kotamarthi, V. R.: Brown carbon: A significant atmospheric
446 absorber of solar radiation?, *Atmos. Chem. Phys.*, 13, 8607-8621, doi:10.5194/acp-13-
447 8607-2013, 2013.
- 448 Flores, J. M., Washenfelder, R. A., Adler, G., Lee, H. J., Segev, L., Laskin, J., Laskin, A.,
449 Nizkorodov, S. A., Brown, S. S., and Rudich, Y.: Complex refractive indices in the near-
450 ultraviolet spectral region of biogenic secondary organic aerosol aged with ammonia, *Phys.*
451 *Chem. Chem. Phys.*, 16, 10629-10642, doi:10.1039/c4cp01009d, 2014.
- 452 Gilardoni, S., Massoli, P., Paglione, M., Giulianelli, L., Carbone, C., Rinaldi, M., Decesari, S.,



- 453 Sandrini, S., Costabile, F., Gobbi, G. P., Pietrogrande, M. C., Visentin, M., Scotto, F., Fuzzi,
454 S., and Facchini, M. C.: Direct observation of aqueous secondary organic aerosol from
455 biomass-burning emissions, *Proc. Natl. Acad. Sci.*, 113, 10013-10018,
456 doi:10.1073/pnas.1602212113, 2016.
- 457 Harrison, M. A. J., Barra, S., Borghesi, D., Vione, D., Arsene, C., and Olariu, R. I.: Nitrated
458 phenols in the atmosphere: a review, *Atmos. Environ.*, 39, 231-248,
459 doi:10.1016/j.atmosenv.2004.09.044, 2005.
- 460 Hecobian, A., Zhang, X., Zheng, M., Frank, N. H., Edgerton, E. S., and Weber, R. J.: Water-
461 soluble organic aerosol material and the light absorption characteristics of aqueous extracts
462 measured over the Southeastern United States, *Atmos. Chem. Phys.*, 10, 5965-5977,
463 doi:10.5194/acp-10-5965-2010, 2010.
- 464 Ho, K. F., Ho, S. S. H., Huang, R. J., Liu, S. X., Cao, J. J., Zhang, T., Chuang, H. C., Chan, C.
465 S., Hu, D., and Tian, L.: Characteristics of water-soluble organic nitrogen in fine
466 particulate matter in the continental area of China, *Atmos. Environ.*, 106, 252-261,
467 doi:10.1016/j.atmosenv.2015.02.010, 2015.
- 468 Huang, R. J., Yang, L., Cao, J., Chen, Y., Chen, Q., Li, Y., Duan, J., Zhu, C., Dai, W., Wang, K.,
469 Lin, C., Ni, H., Corbin, J. C., Wu, Y., Zhang, R., Tie, X., Hoffmann, T., O'Dowd, C., and
470 Dusek, U.: Brown carbon aerosol in urban Xi'an, Northwest China: the composition and
471 light absorption properties, *Environ. Sci. Technol.*, 52, 6825-6833,
472 doi:10.1021/acs.est.8b02386, 2018.
- 473 Iinuma, Y., Böge, O., Gräfe, R., and Herrmann, H.: Methyl-nitrocatechols: atmospheric tracer
474 compounds for biomass burning secondary organic aerosols, *Environ. Sci. Technol.*, 44,
475 8453-8459, doi:10.1021/Es102938a, 2010.
- 476 Jacobson, M. Z.: Isolating nitrated and aromatic aerosols and nitrated aromatic gases as sources
477 of ultraviolet light absorption, *J. Geophys. Res.*, 104, 3527-3542,
478 doi:10.1029/1998jd100054, 1999.
- 479 Kampf, C. J., Jakob, R., and Hoffmann, T.: Identification and characterization of aging products
480 in the glyoxal/ammonium sulfate system - implications for light-absorbing material in
481 atmospheric aerosols, *Atmos. Chem. Phys.*, 12, 6323-6333, doi:10.5194/acp-12-6323-



- 482 2012, 2012.
- 483 Kirillova, E. N., Andersson, A., Han, J., Lee, M., and Gustafsson, Ö.: Sources and light
484 absorption of water-soluble organic carbon aerosols in the outflow from northern China,
485 Atmos. Chem. Phys., 14, 1413-1422, 2014a.
- 486 Kirillova, E. N., Andersson, A., Tiwari, S., Srivastava, A. K., Bisht, S. D., and Gustafsson, Ö.:
487 Water-soluble organic carbon aerosols during a full New Delhi winter: Isotope-based
488 source apportionment and optical properties, J. Geophys. Res. Atmos., 119, 3476–3485,
489 2014b.
- 490 Lambe, A. T., Cappa, C. D., Massoli, P., Onasch, T. B., Forestieri, S. D., Martin, A. T.,
491 Cummings, M. J., Croasdale, D. R., Brune, W. H., Worsnop, D. R., and Davidovits, P.:
492 Relationship between oxidation level and optical properties of secondary organic aerosol,
493 Environ. Sci. Technol., 47, 6349-6357, doi:10.1021/es401043j, 2013.
- 494 Laskin, A., Laskin, J., and Nizkorodov, S. A.: Chemistry of atmospheric brown carbon, Chem.
495 Rev., 115, 4335-4382, doi:10.1021/cr5006167, 2015.
- 496 Lee, H. J., Aiona, P. K., Laskin, A., Laskin, J., and Nizkorodov, S. A.: Effect of solar radiation
497 on the optical properties and molecular composition of laboratory proxies of atmospheric
498 brown carbon, Environ. Sci. Technol., 48, 10217-10226, 2014.
- 499 Lei, Y. L., Shen, Z. X., Wang, Q. Y., Zhang, T., Cao, J. J., Sun, J., Zhang, Q., Wang, L. Q., Xu,
500 H. M., Tian, J., and Wu, J. M.: Optical characteristics and source apportionment of brown
501 carbon in winter PM_{2.5} over Yulin in Northern China, Atmos. Res., 213, 27-33,
502 doi:10.1016/j.atmosres.2018.05.018, 2018.
- 503 Li, G., Bei, N., Tie, X., and Molina, L. T.: Aerosol effects on the photochemistry in Mexico
504 City during MCMA-2006/MILAGRO campaign, Atmos. Chem. Phys., 11, 5169-5182,
505 doi:10.5194/acp-11-5169-2011, 2011.
- 506 Li, Y. J., Huang, D. D., Cheung, H. Y., Lee, A. K. Y., and Chan, C. K.: Aqueous-phase
507 photochemical oxidation and direct photolysis of vanillin - a model compound of methoxy
508 phenols from biomass burning, Atmos. Chem. Phys., 14, 2871-2885, doi:10.5194/acp-14-
509 2871-2014, 2014.
- 510 Lin, P., Aiona, P. K., Li, Y., Shiraiwa, M., Laskin, J., Nizkorodov, S. A., and Laskin, A.:



- 511 Molecular characterization of brown carbon in biomass burning aerosol particles, *Environ.*
512 *Sci. Technol.*, **50**, 11815-11824, doi:10.1021/acs.est.6b03024, 2016.
- 513 Lin, P., Bluvshstein, N., Rudich, Y., Nizkorodov, S. A., Laskin, J., and Laskin, A.: Molecular
514 chemistry of atmospheric brown carbon inferred from a nationwide biomass burning event,
515 *Environ. Sci. Technol.*, **51**, 11561-11570, doi:10.1021/acs.est.7b02276, 2017.
- 516 Lin, P., Fleming, L. T., Nizkorodov, S. A., Laskin, J., and Laskin, A.: Comprehensive Molecular
517 Characterization of Atmospheric Brown Carbon by High Resolution Mass Spectrometry
518 with Electrospray and Atmospheric Pressure Photoionization, *Anal. Chem.*, **90**, 12493-
519 12502, doi:10.1021/acs.analchem.8b02177, 2018.
- 520 Liu, Y., Yan, C. Q., Ding, X., Wang, X. M., Fu, Q. Y., Zhao, Q. B., Zhang, Y. H., Duan, Y. S.,
521 Qiu, X. H., and Zheng, M.: Sources and spatial distribution of particulate polycyclic
522 aromatic hydrocarbons in Shanghai, China, *Sci. Total Environ.*, 584-585, 307-317,
523 doi:10.1016/j.scitotenv.2016.12.134, 2017.
- 524 Lu, C., Wang, X., Li, R., Gu, R., Zhang, Y., Li, W., Gao, R., Chen, B., Xue, L., and Wang, W.:
525 Emissions of fine particulate nitrated phenols from residential coal combustion in China,
526 *Atmos. Environ.*, **203**, 10-17, doi:10.1016/j.atmosenv.2019.01.047, 2019.
- 527 Lu, J. W., Michel Flores, J., Lavi, A., Abo-Riziq, A., and Rudich, Y.: Changes in the optical
528 properties of benzo[a]pyrene-coated aerosols upon heterogeneous reactions with NO₂ and
529 NO₃, *Phys. Chem. Chem. Phys.*, **13**, 6484-6492, doi:10.1039/C0CP02114H, 2011.
- 530 Mohr, C., Lopez-Hilfiker, F. D., Zotter, P., Prevot, A. S. H., Xu, L., Ng, N. L., Herndon, S. C.,
531 Williams, L. R., Franklin, J. P., Zahniser, M. S., Worsnop, D. R., Knighton, W. B., Aiken,
532 A. C., Gorkowski, K. J., Dubey, M. K., Allan, J. D., and Thornton, J. A.: Contribution of
533 nitrated phenols to wood burning brown carbon light absorption in Detling, United
534 Kingdom during winter time, *Environ. Sci. Technol.*, **47**, 6316-6324,
535 doi:10.1021/es400683v, 2013.
- 536 Moise, T., Flores, J. M., and Rudich, Y.: Optical properties of secondary organic aerosols and
537 their changes by chemical processes, *Chem. Rev.*, **115**, 4400-4439, doi:10.1021/cr5005259,
538 2015.
- 539 Mok, J., Krotkov, N. A., Arola, A., Torres, O., Jethva, H., Andrade, M., Labow, G., Eck, T. F.,



- 540 Li, Z., Dickerson, R. R., Stenchikov, G. L., Osipov, S., and Ren, X.: Impacts of brown
541 carbon from biomass burning on surface UV and ozone photochemistry in the Amazon
542 Basin, *Sci. Rep.*, 6, 36940, doi:10.1038/srep36940, 2016.
- 543 Moschos, V., Kumar, N. K., Daellenbach, K. R., Baltensperger, U., Prévôt, A. S. H., and El
544 Haddad, I.: Source Apportionment of Brown Carbon Absorption by Coupling Ultraviolet-
545 Visible Spectroscopy with Aerosol Mass Spectrometry, *Environ. Sci. Tech. Let.*, 5, 302-
546 308, doi:10.1021/acs.estlett.8b00118, 2018.
- 547 Nguyen, T. B., Laskin, A., Laskin, J., and Nizkorodov, S. A.: Brown carbon formation from
548 ketoaldehydes of biogenic monoterpenes, *Faraday Discuss.*, 165, 473-494,
549 doi:10.1039/C3FD00036B, 2013.
- 550 Ni, H. Y., Huang, R. J., Cao, J. J., Liu, W. G., Zhang, T., Wang, M., Meijer, H. A. J., and Dusek,
551 U.: Source apportionment of carbonaceous aerosols in Xi'an, China: insights from a full
552 year of measurements of radiocarbon and the stable isotope ^{13}C , *Atmos. Chem. Phys.*, 18,
553 16363-16383, doi:10.5194/acp-18-16363-2018, 2018.
- 554 Paatero, P.: Least squares formulation of robust non-negative factor analysis, *Chemom. Intell.*
555 *Lab.*, 37, 23-35, doi:10.1016/S0169-7439(96)00044-5, 1997.
- 556 Park, R. J., Kim, M. J., Jeong, J. I., Yooun, D., and Kim, S.: A contribution of brown carbon
557 aerosol to the aerosol light absorption and its radiative forcing in East Asia, *Atmos.*
558 *Environ.*, 44, 1414-1421, doi:10.1016/j.atmosenv.2010.01.042, 2010.
- 559 Park, S., Yu, G. H., and Lee, S.: Optical absorption characteristics of brown carbon aerosols
560 during the KORUS-AQ campaign at an urban site, *Atmos. Res.*, 203, 16-27,
561 doi:10.1016/j.atmosres.2017.12.002, 2018.
- 562 Ram, K., Sarin, M. M., and Tripathi, S. N.: Temporal trends in atmospheric $\text{PM}_{2.5}$, PM_{10} ,
563 elemental carbon, organic carbon, water-soluble organic carbon, and optical properties:
564 impact of biomass burning emissions in the Indo-Gangetic Plain, *Environ. Sci. Technol.*,
565 46, 686-695, doi:10.1021/es202857w, 2012.
- 566 Samburova, V., Connolly, J., Gyawali, M., Yatavelli, R. L. N., Watts, A. C., Chakrabarty, R. K.,
567 Zielinska, B., Moosmüller, H., and Khlystov, A.: Polycyclic aromatic hydrocarbons in
568 biomass-burning emissions and their contribution to light absorption and aerosol toxicity,



- 569 Sci. Total Environ., 568, 391-401, doi:10.1016/j.scitotenv.2016.06.026, 2016.
- 570 Shapiro, E. L., Szprengiel, J., Sareen, N., Jen, C. N., Giordano, M. R., and McNeill, V. F.: Light-
571 absorbing secondary organic material formed by glyoxal in aqueous aerosol mimics,
572 Atmos. Chem. Phys., 9, 2289-2300, doi:10.5194/acp-9-2289-2009, 2009.
- 573 Smith, J. D., Kinney, H., and Anastasio, C.: Phenolic carbonyls undergo rapid aqueous
574 photodegradation to form low-volatility, light-absorbing products, Atmos. Environ., 126,
575 36-44, doi:10.1016/j.atmosenv.2015.11.035, 2016.
- 576 Srinivas, B., and Sarin, M. M.: Light-absorbing organic aerosols (brown carbon) over the
577 tropical Indian Ocean: impact of biomass burning emissions, Environ. Res. Lett., 8,
578 044042, doi:10.1088/1748-9326/8/4/044042, 2013.
- 579 Teich, M., van Pinxteren, D., Wang, M., Kecorius, S., Wang, Z., Müller, T., Mocnik, G., and
580 Herrmann, H.: Contributions of nitrated aromatic compounds to the light absorption of
581 water-soluble and particulate brown carbon in different atmospheric environments in
582 Germany and China, Atmos. Chem. Phys., 17, 1653-1672, doi:10.5194/acp-17-1653-2017,
583 2017.
- 584 Wang, G. H., Kawamura, K., Lee, S., Ho, K. F., and Cao, J. J.: Molecular, seasonal, and spatial
585 distributions of organic aerosols from fourteen Chinese cities, Environ. Sci. Technol., 40,
586 4619-4625, doi:10.1021/es060291x, 2006.
- 587 Wang, J. Z., Ho, S. S. H., Huang, R. J., Gao, M. L., Liu, S. X., Zhao, S. Y., Cao, J. J., Wang, G.
588 H., Shen, Z. X., and Han, Y. M.: Characterization of parent and oxygenated-polycyclic
589 aromatic hydrocarbons (PAHs) in Xi'an, China during heating period: An investigation of
590 spatial distribution and transformation, Chemosphere, 159, 367-377,
591 doi:10.1016/j.chemosphere.2016.06.033, 2016.
- 592 Wang, L. W., Wang, X. F., Gu, R. R., Wang, H., Yao, L., Wen, L., Zhu, F. P., Wang, W. H., Xue,
593 L. K., Yang, L. X., Lu, K. D., Chen, J. M., Wang, T., Zhang, Y. H., and Wang, W. X.:
594 Observations of fine particulate nitrated phenols in four sites in northern China:
595 concentrations, source apportionment, and secondary formation, Atmos. Chem. Phys., 18,
596 4349-4359, doi:10.5194/acp-18-4349-2018, 2018.
- 597 Washenfelder, R. A., Attwood, A. R., Brock, C. A., Guo, H., Xu, L., Weber, R. J., Ng, N. L.,



- 598 Allen, H. M., Ayres, B. R., Baumann, K., Cohen, R. C., Draper, D. C., Duffey, K. C.,
599 Edgerton, E., Fry, J. L., Hu, W. W., Jimenez, J. L., Palm, B. B., Romer, P., Stone, E. A.,
600 Wooldridge, P. J., and Brown, S. S.: Biomass burning dominates brown carbon absorption
601 in the rural southeastern United States, *Geophys. Res. Lett.*, doi:10.1002/2014GL062444,
602 42, 653-664, 2015.
- 603 Xie, M. J., Chen, X., Hays, M. D., Lewandowski, M., Offenberg, J., Kleindienst, T. E., and
604 Holder, A. L.: Light absorption of secondary organic aerosol: composition and
605 contribution of nitroaromatic compounds, *Environ. Sci. Technol.*, 51, 11607-11616,
606 doi:10.1021/acs.est.7b03263, 2017.
- 607 Xie, M. J., Chen, X., Holder, A. L., Hays, M. D., Lewandowski, M., Offenberg, J. H.,
608 Kleindienst, T. E., Jaoui, M., and Hannigan, M. P.: Light absorption of organic carbon and
609 its sources at a southeastern U.S. location in summer, *Environ. Pollut.*, 244, 38-46,
610 doi:10.1016/j.envpol.2018.09.125, 2019.
- 611 Yan, C. Q., Zheng, M., Sullivan, A. P., Bosch, C., Desyaterik, Y., Andersson, A., Li, X. Y., Guo,
612 X. S., Zhou, T., Gustafsson, O., and Collett Jr, J. L.: Chemical characteristics and light-
613 absorbing property of water-soluble organic carbon in Beijing: Biomass burning
614 contributions, *Atmos. Environ.*, 121, 4-12, doi:10.1016/j.atmosenv.2015.05.005, 2015.
- 615 Yan, C. Q., Zheng, M., Bosch, C., Andersson, A., Desyaterik, Y., Sullivan, A. P., Collett, J. L.,
616 Zhao, B., Wang, S. X., He, K. B., and Gustafsson, Ö.: Important fossil source contribution
617 to brown carbon in Beijing during winter, *Sci. Rep.*, 7, 43182, doi:10.1038/srep43182,
618 2017.
- 619 Zhang, X., Lin, Y.-H., Surratt, J. D., and Weber, R.: Sources, composition and absorption
620 Ångström exponent of light-absorbing organic components in aerosol extracts from the
621 Los Angeles Basin, *Environ. Sci. Technol.*, 47, 3685-3693, doi:10.1021/es305047b, 2013.
- 622 Zhang, Y., Forrister, H., Liu, J., Dibb, J., Anderson, B., Schwarz, J. P., Perring, A. E., Jimenez,
623 J. L., Campuzano-Jost, P., Wang, Y., Nenes, A., and Weber, R. J.: Top-of-atmosphere
624 radiative forcing affected by brown carbon in the upper troposphere, *Nat. Geosci.*, 10, 486-
625 489, doi:10.1038/NGEO2960, 2017a.
- 626 Zhang, Y., Xu, J., Shi, J., Xie, C., Ge, X., Wang, J., Kang, S., and Zhang, Q.: Light absorption



627 by water-soluble organic carbon in atmospheric fine particles in the central Tibetan Plateau,
628 Environ. Sci. Pollut. Res., 24, 21386–21397, doi:10.1007/s11356-017-9688-8, 2017b.

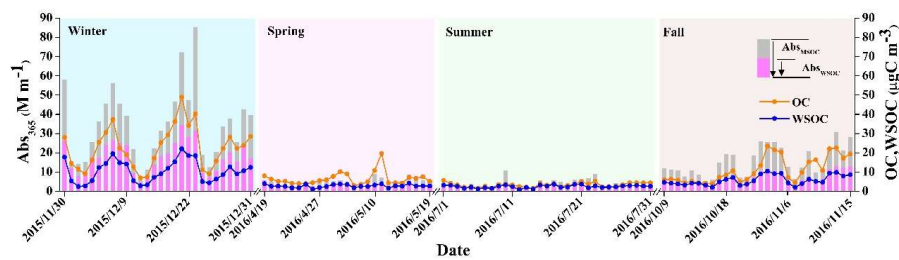
629 Zhong, M., and Jang, M.: Dynamic light absorption of biomass-burning organic carbon
630 photochemically aged under natural sunlight, Atmos. Chem. Phys., 14, 1517-1525, 2014.

631 Zhu, C. S., Cao, J. J., Huang, R. J., Shen, Z. X., Wang, Q. Y., and Zhang, N. N.: Light absorption
632 properties of brown carbon over the southeastern Tibetan Plateau, Sci. Total Environ., 625,
633 246-251, doi:10.1016/j.scitotenv.2017.12.183, 2018.



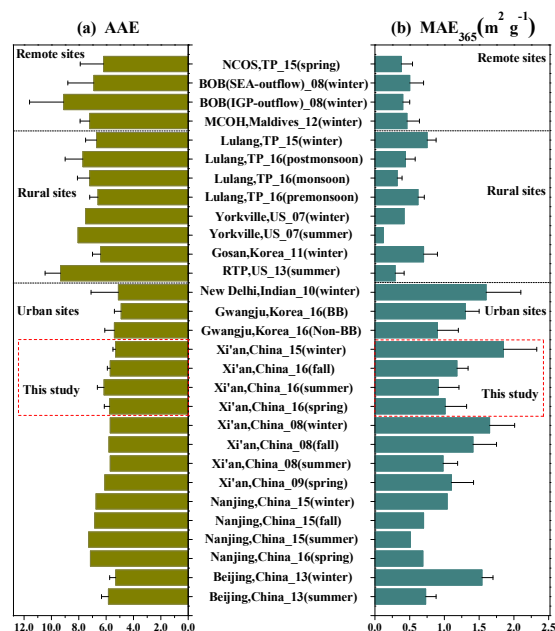
634 **Table 1.** Annual and seasonal mean contributions of measured PAHs, NACs and MOPs to
 635 methanol-soluble BrC light absorption at 365 nm. Hyphens denote the measured value of more
 636 than one third of the samples is below the detection limit.

Compounds	MAE ₃₆₅ (m ² g ⁻¹)	Contribution to BrC light absorption at 365 nm (%)				
		Annual	Spring	Summer	Fall	Winter
Fluoranthene (FLU)	4.25	0.11	0.05	0.02	0.05	0.15
Pyrene (PYR)	0.46	0.01	0.00	0.00	0.01	0.01
Chrysene (CHR)	0.00	0.00	0.00	0.00	0.00	0.00
Benzo(a)anthracene (BaA)	2.06	0.04	0.01	0.01	0.02	0.05
Benzo(a)pyrene (BaP)	9.31	1.04	0.76	0.39	1.16	1.10
Benzo(b)fluoranthene (BbF)	4.10	0.17	0.14	0.07	0.17	0.18
Benzo(k)fluoranthene (BkF)	3.47	0.04	0.03	0.02	0.04	0.04
Indeno[1,2,3-cd]pyrene (IcdP)	4.68	0.51	0.50	0.24	0.71	0.46
Benzo(ghi)perylene (BghiP)	8.95	0.29	0.28	0.16	0.41	0.26
9,10-Anthracenequinone (9,10AQ)	0.28	0.01	0.00	0.00	0.00	0.01
Benzanthrone (BEN)	6.13	0.11	0.08	0.05	0.11	0.12
Benzo[b]fluoren-11-one (BbF11O)	1.89	0.02	0.02	0.01	0.02	0.03
4-Nitrophenol (4NP)	2.17	0.08	0.06	0.02	0.05	0.10
4-Nitro-1-naphthol (4N1N)	9.71	-	-	-	-	0.03
2-Methyl-4-nitrophenol (2M4NP)	2.81	0.03	0.01	0.01	0.01	0.04
3-Methyl-4-nitrophenol (3M4NP)	2.65	0.02	0.01	0.00	0.01	0.03
2,6-Dimethyl-4-nitrophenol (2,6DM4NP)	3.27	-	-	-	-	0.01
4-Nitrocatechol (4NC)	7.91	0.27	0.05	0.03	0.20	0.35
3-Methyl-5-nitrocatechol (3M5NC)	5.77	-	-	-	0.05	0.11
4-Methyl-5-nitrocatechol (4M5NC)	7.29	-	-	-	0.06	0.13
3-Nitrosalicylicacid (3NSA)	3.86	-	-	-	-	0.01
5-Nitrosalicylicacid (5NSA)	3.36	0.03	0.01	0.02	0.04	0.02
Syringyl acetone (SyA)	0.25	0.01	0.01	0.00	0.01	0.01
Vanillin (VAN)	8.17	0.01	0.00	0.00	0.00	0.01
Vanillic acid (VaA)	0.66	0.00	0.00	0.00	0.00	0.00
Total	103.46	2.80	2.02	1.05	3.13	3.26



637

638 **Figure 1.** Time series of the light absorption coefficient of water-soluble and methanol-soluble
639 BrC at 365 nm ($Abs_{365,WSOC}$ and $Abs_{365,MSOC}$, respectively), as well as OC and WSOC
640 concentrations.



641

642 **Figure 2.** Comparison of AAE (left column) and MAE₃₆₅ (right column) values of water-soluble
 643 BrC at remote sites (Srinivas and Sarin, 2013; Bosch et al., 2014; Zhang et al., 2017b), rural
 644 sites (Hocobian et al., 2010; Kirillova et al., 2014a; Zhu et al., 2018; Xie et al., 2019) and urban
 645 sites (Kirillova et al., 2014b; Yan et al., 2015; Chen et al., 2018; Huang et al., 2018; Park et al.,
 646 2018).

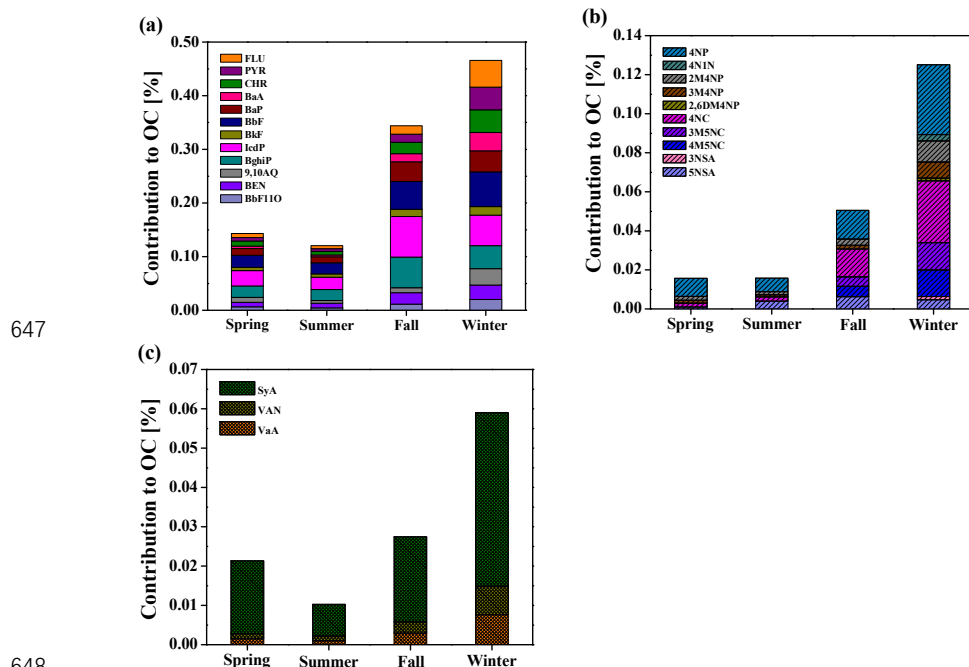
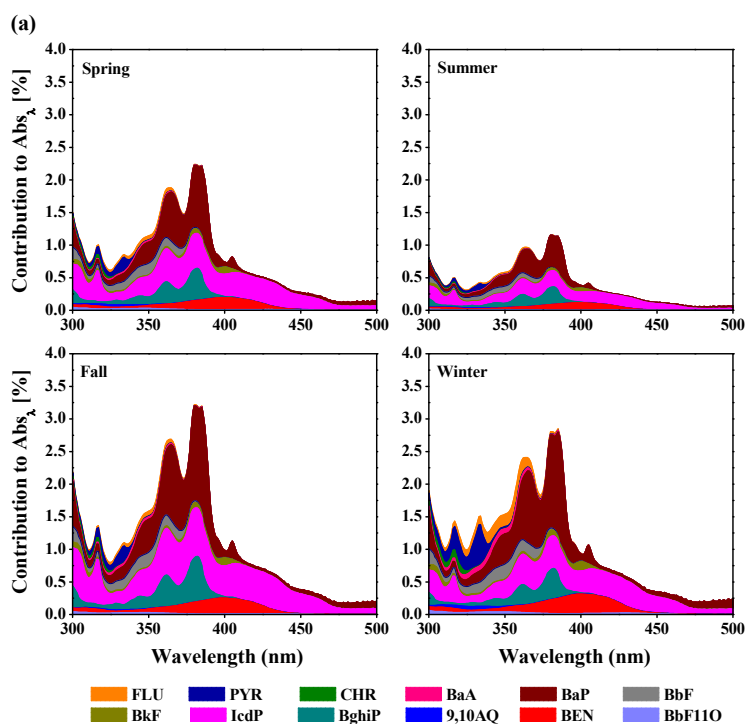
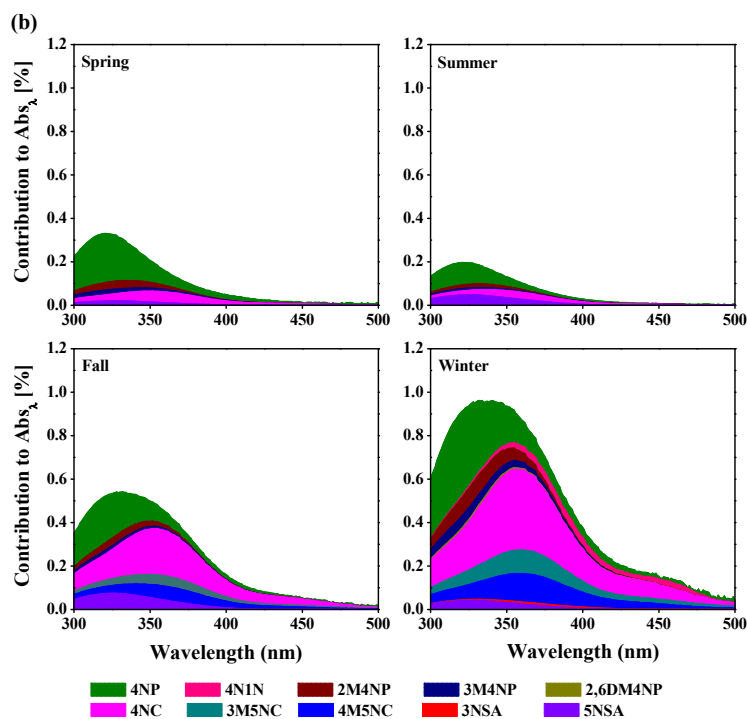


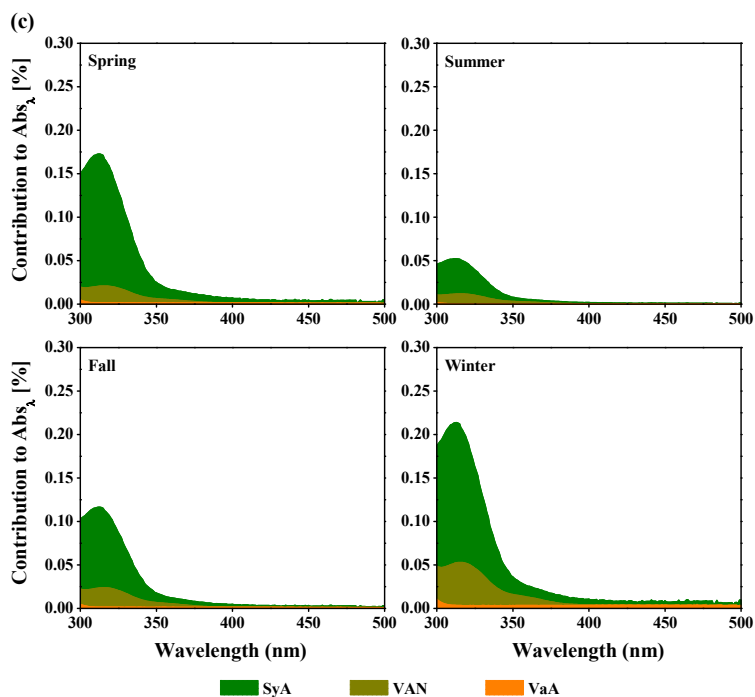
Figure 3. Contributions of (a) PAHs, (b) NACs, and (c) MOPs carbon mass concentrations to the total OC concentrations.



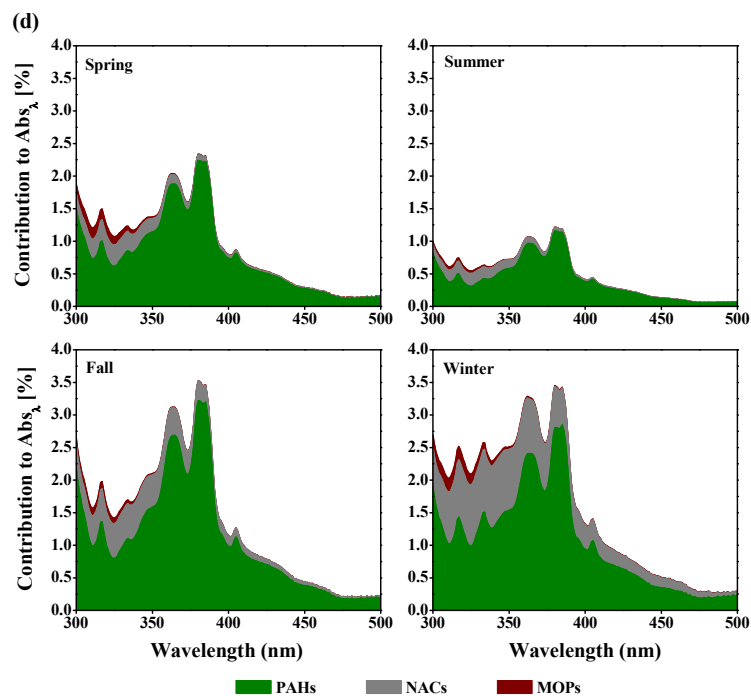
653



654



655

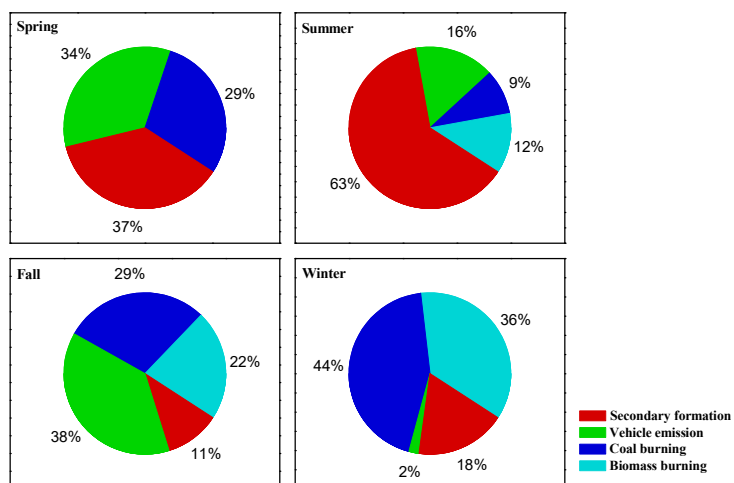


656

657 **Figure 4.** Light absorption contributions of (a) PAHs, (b) NACs, (c) MOPs and (d) total



658 measured chromophores to Abs_{MSOC} over the wavelength range of 300 to 500 nm in spring,
659 summer, fall and winter.
660



661

662 **Figure 5.** Contributions of the major sources to $Abs_{365,MSOC}$ in Xi'an during spring, summer, fall

663 and winter.